Journal of Ceramic Processing Research. Vol. 1, No. 2, pp. 109~114 (2000)

J O U R N A L O F
Ceramic Processing Research

Atomic ordering reaction and associated variation of magnetic coercivity of oriented $L1_0$-FePt nanoparticles

Kazuhisa Sato*, Bo Bian[a] and Yoshihiko Hirotsu

The Institute of Scientific and Industrial Reseach, Osaka University, 8-1 Mihogaoka, Ibaraki, Osaka 5670047, Japan

[a]Presently at: Carnegie Mellon Univ., Pittsburgh, PA 15213-3890, USA

Atomically ordered FePt nanoparticles ($L1_0$-type structure) covered with amorphous (a-) Al_2O_3 have been fabricated. In this process, Fe particles were deposited on Pt "seed" particles which were epitaxially grown on (100) NaCl or MgO substrates. Annealing the a-Al_2O_3/Fe/Pt films at temperatures higher than 773 K leads to a formation of ordered nanoparticles with mutual fixed orientation in a monolayer form. Three variant ordered domains of the tetragonal $L1_0$ structure coexisted in a single nm-sized FePt particle, even in a particle as small as 7 nm. According to in-situ electron diffraction study, the degree of order of the ordered structure started to increase on annealing at 773 K and almost saturated on annealing at 873 K for 16 h. The magnetic coercivity varied depending on the particle size and the degree of order in the $L1_0$ structure formation. The perpendicular coercivity exceeded the in-plane one during the annealing. The in-plane coercivities of FePt nanoparticles measured both parallel to $[100]_{MgO}$ and $[010]_{MgO}$ directions were almost equal in numerical value. These results reflect the ordered domain formation process and the volume fraction of the domains. Remanent magnetization decay measured for the in-plane magnetization revealed a magnetic relaxation with the type of magnetic dipolar interaction between the FePt particles.

Key words: Atomic ordering, $L1_0$-FePt, Amorphous Al_2O_3, HRTEM, Hard magnetism, High-density recording, Thermal fluctuation, Remanent magnetization decay.

Introduction

Recently, the magnetic recording density has become higher year by year and reached nearly the maximum value (around 1 Gbit/in^2 [1]) for the conventional recording media with continuous magnetic thin films. It is predicted that the density of magnetic recording will reach to 10 to 100 Gbits/in^2 [2-4] during the years between 2001 and 2006 according to today's rate of progress [4]. The grain sizes of recording media have been decreasing to increase the recording density. As the candidates for near future high-density recording media, films including FePt and CoPt ordered alloy nano particulates, called "nano-granular films" have been attracting much attention in recently [5-7]. These alloy nanoparticles include atomic ordering reactions from disordered fcc phase to ordered $L1_0$ phase [8] (CuAu I-type structure) in their fabrication processes. The ordered structure of these alloys have a large magnetocrystalline anisotropy energy as high as 10^6 to 10^7 J/m^3 [9-10], which is one hundred times larger than that of bcc-Fe. When the volume of the magnetic particles decreased, the thermal fluctuation of magnetization affect the magnetization of particles, and cause the disappearance of memorized information. Shimatsu *et al*. discussed the effect of thermal fluctuation of magnetic moment on the ordered $L1_0$-FePt nanogranular film [12]. The particle morphology, size, crystallographic orientation and inter-particle distance are strongly dependent on the fabrication process, and these parameters affect their magnetic properties largely. For example, the magnetic coercivity of Fe nanoparticles shows peculiar dependence on the inter-particle distance [13], and the partide size [14]. From the practical viewpoints as the longitudinal magnetic recording media, the easy axis of the material, which is usually related to their crystallographic structure, have to be oriented parallel to the film plane. Also, as the magneto-optical or perpendicular recording media, the easy axis has to be aligned perpendicular to the film plane. However few studies have reported the orientation control in nano-particulate systems, in spite of many approaches for epitaxial growth performed in FePt and CoPt thin continuous films [11, 15-20]. The present authors have reported the structure and magnetic properties of oriented $L1_0$-FePt nanoparticles on amorphous (a-) Al_2O_3 thin film [21-24]. In this paper, we report our recent study of FePt nanoparticles, especially, on their atomic ordering reactions and the related variation of magnetic properties.

Experimental Procedures

Thin films of oriented FePt nanoparticles covered with

*Corresponding author:
Tel : +81-6-6879-8431
Fax: +81-6-6879-8434
E-mail: sato@sanken.osaka-u.ac.jp

amorphous Al_2O_3 were fabricated using an electron-beam evaporation technique in a high-vacuum chamber with a base pressure of approximately 3×10^{-7} Pa. The process took advantage of the overgrowth of bcc-Fe on fcc-Pt "seed" particles, which were epitaxially grown on (100) NaCl and MgO substrates kept at 673 K during the deposition [21-22], and also of an ordering reaction between Fe and Pt on annealing at temperatures higher than 773 K. A quartz thickness monitor was attached in the chamber to estimate the average thickness of the deposited layers. First, Pt particles were deposited with a rate of 0.1 to 0.5 nm/min on both of the NaCl and MgO substrates set side by side and kept at 673 K. Successively, Fe was deposited onto the substrates at a deposition rate of 0.3 to 1.0 nm/min. In order to protect the deposited Fe from oxidization, a cover layer of a-Al_2O_3 with a thickness larger than 4 nm was deposited without breaking vacuum. The averaged thicknesses of the "seed" Pt particle layers were set to be 0.5 to 1.5 nm and that of Fe ranged from 0.5 to 3.5 nm. A part of the NaCl (100) substrate with the as-deposited or after-annealed films was immersed in distilled water and the deposited films removed were mounted onto copper microgrids for later transmission electron microscopy (TEM) observations with 200 and 300 kV electron microscopes. Annealing of the specimens were mainly performed in a vacuum furnace with a pressure less than 2×10^{-5} Pa at 873 K for several hours. Because of the epitaxial relations between the substrate and Pt ($<011>_s$ //$<011>_{Pt}$, $\{100\}_s$ //$\{100\}_{Pt}$), and between Pt and Fe ($<100>_{Fe}$//$<100>_{Pt}$, $\{011\}_{Fe}$//$\{010\}_{Pt}$) [21-22], the $L1_0$-FePt nanoparticles observed by TEM were found to be grown mutually under a fixed orientation. The atomic ordering reactions were studied by in-situ TEM observation using a specimen heating stage. The composition analysis of the specimen was done by energy dispersive X-ray spectroscopy (EDS) apparatus, which was attached to the TEM. Magnetization hysteresis loops of the films on NaCl and MgO substrates were measured with a superconducting quantum interference devise (SQUID) magnetometer in the temperature range from 10 to 300 K. No appreciable difference between magnetic data from the films on NaCl and MgO was observed. Thermoremanent magnetization decay was also measured using SQUID as follows. At first, we applied the field of 10 kOe parallel to the film plane and abruptly removed it to 0, followed by measuring the decay curve for around 10^3 min.

Results and Discussion

Structural change by atomic ordering

Figure 1 shows three examples of selected area electron diffraction (SAED) patterns taken from an a-Al_2O_3/Fe (44 at.%)/Pt (56 at.%) film at 300, 773 and 873 K in the course of annealing in TEM. These SAED patterns were received using imaging plates. Each of these patterns was taken after keeping 10 min at each temperature. In the pattern for the as-deposited (300 K) condition, fcc-Pt and bcc-Fe coexists satisfying the epitaxial orientation relationship [21-22] mentioned in the experimental procedures. A halo-pattern from the a-Al_2O_3 can be seen as the background. At 773 K, weak superlattice reflections started to be seen, though weak spots from the residual bcc-Fe are still observed. At 873 K, superlattice reflections became strong, and reflections from the residual bcc-Fe disappeared. This result indicates that the alloying process of Pt and Fe, and the atomic ordering process from disordered Fe-Pt to the ordered $L1_0$-FePt structure (CuAu I-type) occurred almost simultaneously. The change of SAED intensity profiles with the annealing temperature are shown in Fig. 2, which were measured along $[001]^*_{FePt}$

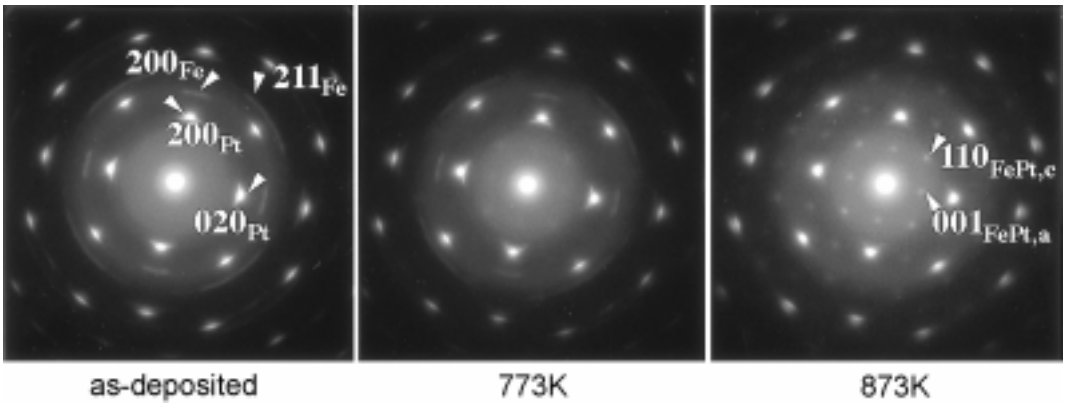

Fig. 1. Three examples of SAED patterns of an a-Al_2O_3/Fe (44 at.%)/Pt (56 at.%) film at 300, 773 and 873 K extracted from the in-situ observation in the temperature range from 300 to 873 K. The superlattice reflections gradually appeared with increasing the annealing temperature, and on the contrary, the reflections from the residual bcc-Fe disappeared simultaneously. The spotty diffraction patterns mean the existence of mutual orientation relationships between the FePt nanocrystallites (fcc-Pt and bcc-Fe at 300 K). In the pattern for 873 K, the superreflections $110_{FePt,\,c}$ and $001_{FePt,\,a}$ come from the structural domains with c-axis normal and parallel to the film, respectively.

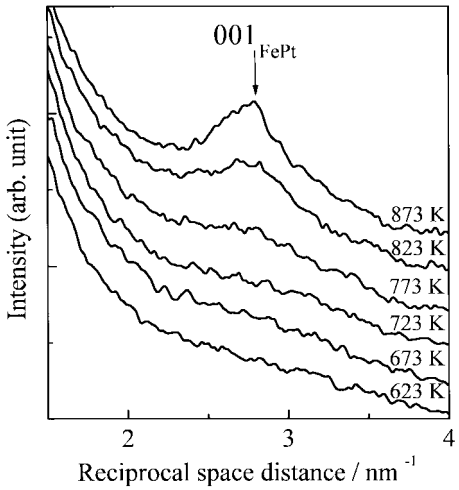

Fig. 2. The SAED intensity profiles for different temperatures measured along the $[001]^*_{FePt}$ direction in the pattern. Superlattice reflection position is shown by the arrow in the figure. Intensity of the ordered reflection 001_{FePt} appeared at 773 K and gradually enhanced with increasing the annealing temperature.

direction in the pattern. A broad peak of superlattice reflection can be seen above 773 K in Fig. 2. Similarly, a broad peak of superlattice reflection was visible above 773 K in the profiles measured along $[110]^*_{FePt}$ direction.

Figure 3 shows the annealing time dependence of diffracted beam intensity ratio of 110 superlattice reflection to 220 fundamental reflection obtained by in-situ SAED observation performed at 873 K using the same specimen as in Fig. 1 and 2 (Fe-56 at.% Pt). The measurement error represents the standard deviation of measured intensities at each data point. The particles observed by TEM did not coalesce even after the temperature reached at 873 K. At the initial stage of

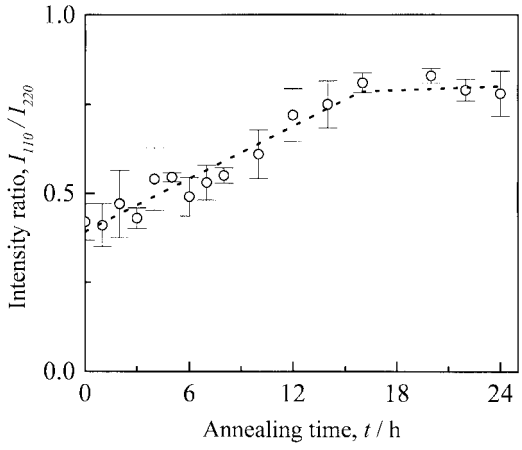

Fig. 3. Variation of intensity ratio of 110 superlattice reflection to 220 fundamental one against the annealing time under 873 K. During the annealing, the specimen thickness could be regarded as constant because of after no particle cohesion on annealing. The increase of 110 reflection intensity was saturated after 16 h annealing.

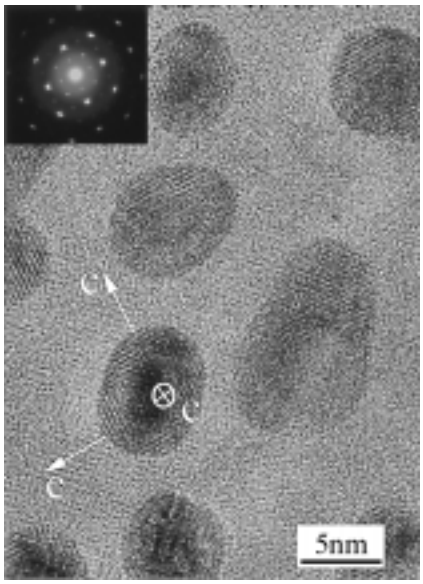

Fig. 4. Lattice fringe images of the FePt nanoparticles and the corresponding SAED pattern for an a-Al_2O_3/Fe (40 at.%)/Pt (60 at.%) film after annealing at 873 K for 1 h. Ordered FePt particles with mean sizes of 8 nm are homogeneously dispersed. Also the ordered domain structures can be seen in the particles. In each particle, the central region corresponds to the domain with the c-axis normal to the film plane and the outer regions corresponds to the domains with the c-axes parallel to the film plane.

annealing, the intensity ratio of 110 to 220 increased linearly, followed by the saturation after about 16 h. Since the dynamical effect in electron diffraction often makes the quantitative interpretation of diffraction intensities difficult. It was difficult to evaluate the accurate long-range order parameters from the SAED patterns. However, since the particles did not change their external shape appreciably during the aging mentioned above, the particle thickness must be almost constant during the annealing. So the saturation of the I_{110}/I_{220} ratio in Fig. 3 can be regarded as the end of ordering reaction. This data is useful for us to decide the appropriate annealing time for sufficient ordering.

In this study, we fabricated various sizes of FePt nanoparticles with average sizes from 8 nm to 20 nm. Figure 4 shows the FePt nanoparticles fabricated with the mean sizes of 8 nm. We have reported in our previous work that three-variant ordered crystalline domains of the $L1_0$ phase could coexist even in nano-sized FePt nanoparticles [21-22]. Such ordered variants can also be seen in small particles even as small as 7 nm in the middle of Fig. 5. This result could be explained by the equivalent chance for nucleation and growth of domains with the three variant crystallographic orientations on the substrate. The easy axis of magnetization in the $L1_0$-FePt structure is c-axis, so the existence of these ordered domains would greatly affect the magnetization process and magnetic properties of the particles. The reason why such domains coexist irrespective of energetically unfavorable situation is unknown at this

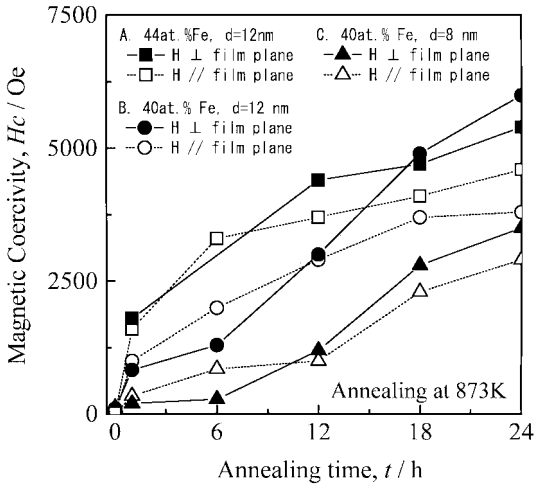

Fig. 5. Variation of magnetic coercivity against the annealing time under 873 K for two kinds of specimen with different mean particle diameters. The coercivities both normal and parallel to the film plane are enhanced with increasing the annealing time, though their coercive forces are reversed after annealing for 10 h.

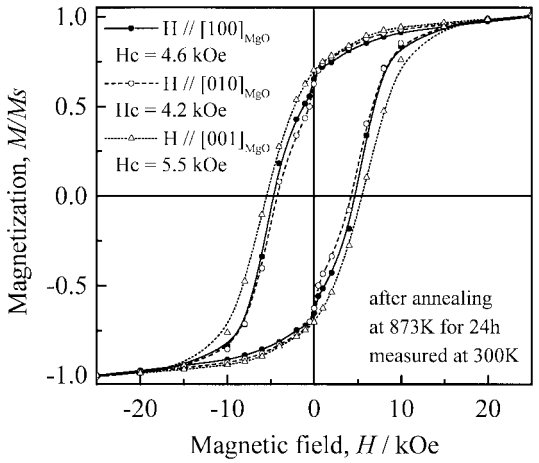

Fig. 6. Typical magnetization vs. magnetic field (M-H) loops for a-Al_2O_3/Fe (44 at.%)/Pt (56 at.%)/MgO(100) films measured at 300 K after annealing at 873 K for 24 h. These three loops were measured using the applied field parallel to the three equivalent principle axes of MgO substrate. The perpendicular coercivity slightly exceeded both of the plane coercivities.

moment.

Variation of magnetic properties due to atomic ordering

Annealing time dependence of coercivities was plotted in Fig. 5. The data marked by square (sample-A) were obtained from the same specimen as observed in Fig. 1 to 3 (mean particle diameter: 12 nm, mean composition: Fe-56 at.% Pt). Another data points marked by circles (sample-B) and triangles (sample-C) were obtained from the specimens with the mean particle sizes of 12 and 8 nm, respectively. Both of them had the averaged concentration of Fe-60 at.% Pt. Coercivities of these specimens showed a similar tendency to the annealing time. At the initial stage of annealing (< 10 h), the in-plane coercivities were larger than the perpendicular one, however, this relationship was reversed when annealed longer than 10 to 12 h. It is considered that the large enhancement of coercivity on annealing is due to the atomic ordering from cubic to tetragonal phase with the higher magnetocrystalline anisotropy. The reversal of the gradient of coercivity change with annealing time must be related to a reversal of volume fractional change of the variant structural domains, the volume of the domain with the c-axis normal to the film plane becomes larger than either of the volume of domain with the c-axis parallel to the film plane. The coercivity change of sample-A on annealing must be closely related to the increase of degree of order of $L1_0$-structure as seen in Fig. 3. However, for the perpendicular and in-plane magnetizations in sample-B and -C, the coercivity reversal was clearly observed after 12 h annealing, and after the reversal, the coercivity difference for the smaller particles is smaller compared with that for the larger particles. So it is considered that the alloy concentration and particle size affect the atomic ordering process and the ordering domain formation. The smallest averaged particle size with a high coercivity (3.5 kOe) obtained so far was 8 nm after annealing at 873 K for 24 h (see solid triangles in Fig. 5).

Figure 6 shows the applied field direction dependence on the hysteresis loop for the specimen with mean particle diameter of 12 nm and the composition of Fe-56 at.% Pt after annealing at 873 K for 24 h. Under the epitaxial orientation relationship, three variants of $L1_0$-domains are epitaxially grown on the MgO substrate. So we induced the field parallel to the direction of $[100]_{MgO}$, $[010]_{MgO}$, these are ("in-plane" direction), and also to $[001]_{MgO}$ (perpendicular direction). The perpendicular coercivity exceeded the in-plane one and the in-plane coercivities measured both parallel to $[100]_{MgO}$ and $[010]_{MgO}$ were almost the same. This result can be expected by the existence of three kinds of variant structural domains mentioned above. From the shape and the squareness of M-H loops with three different magnetic field directions shown in Fig. 6, it is found that the easy axis directions of the film are along the three applied magnetic fields.

Effect of thermal fluctuation on magnetic properties

We studied the temperature dependence of coercivity, since it is expected that the lower the temperature, the smaller the thermal fluctuation becomes. The ratios of coercivities measured at 300 and 10 K (*Hc* (300 K)/*Hc* (10 K)) are presented in Fig. 7 for three specimens with different particle sizes (8 to 14 nm), but have the same averaged composition (Fe-60 at.% Pt) and the same packing density around 0.3 to 0.4. All these specimens were annealed at 873 K for 1 h after the deposition, and are supposed to have almost the same ordered structures. In case of the specimen with sufficiently

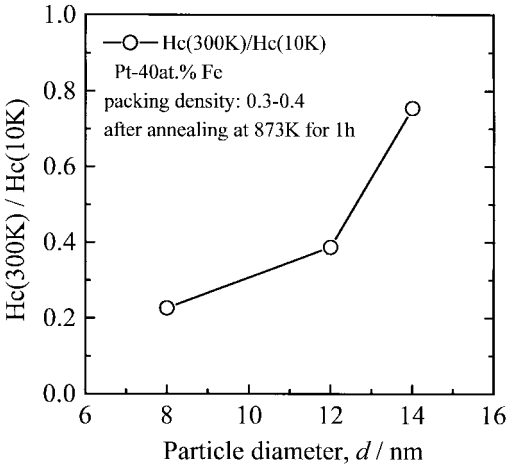

Fig. 7. Mean particle size dependence of coercivity ratio measured at 300 K and 10 K. In case of the specimen with sufficiently large particle diameter, this ratio ought to be near unity. However, in case of nanoparticles with small sizes, this ratio would decrease below unity, depending on the magnitude of thermal fluctuation, which depends on the particle volume.

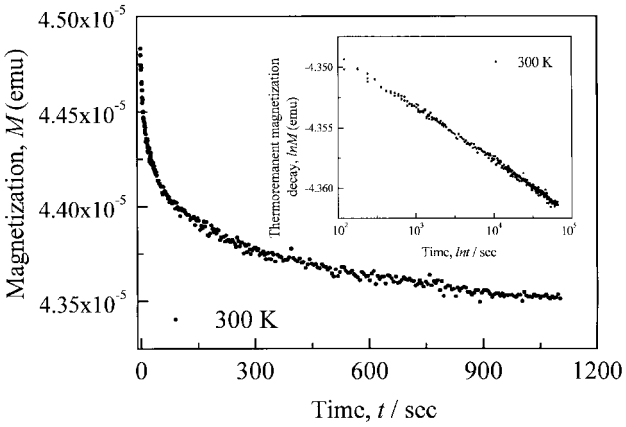

Fig. 8. Remanent magnetization decay curve measured at 300 K with the specimen used in measurement shown in Fig. 7 (a-Al_2O_3/Fe (44 at.%)/Pt (56 at.%)/MgO (100), after annealing at 873 K for 24 h). The residual magnetization decreased with time and saturated after 10^3 min. Their total decay value is about 3%. The curve represented by log-log scale is shown in the inset.

large particle diameter, the ratio (*Hc* (300 K)/*Hc* (10 K)) must be near unity, since the thermal agitation would not affect it seriously because of the thermal stability owing to the high magnetocrystalline anisotropy. However, in case of nanoparticles with small sizes, this ratio would decrease far below unity, depending on the magnitude of thermal fluctuation. Especially in the case of annealing time for 1 h, the ratio rapidly decreased with decreasing the particle diameter, and reached 0.2 for the size of 8 nm. These results strongly suggest the size-dependence of thermal fluctuation for the present FePt nanoparticles, especially for the particle size below about 10 nm.

In order to investigate the correlation of magnetic interaction between the particles, the thermoremanent magentization decay curve was measured at 300 K with the specimen used in the measurement shown in Fig. 6 (a-Al_2O_3/Fe (44at.%)/Pt (56at.%)/MgO (100)). In Fig. 8, the residual magnetization decreased with time and saturated after 10^3 min. Their total decay value was about 3%. This decay curve showed the peculiar time dependence different from the Néel model [25] for non-interacting isolated particles, which represents the magentization decay as

$$M_r(t)=M_0e^{-t/\tau} \quad (1)$$

, where $M_r(t)$ is the time dependent remanent magentization, M_0 the initial remanent magnetization, t the time and τ the relaxation time. This expression can be rewritten as $\log M_r(t) \propto -t$. However, our result showed the log-log type time dependence, that is,

$$\log M_r(t) \propto -\log t \quad (2)$$

as shown in the inset of Fig. 8. Relaxation relationships different from Néel model were discussed both theoretically [26] and experimentally [27] from the viewpoint of intergranular magnetic interactions. Our recent study indicated the existence of weak intergranular magnetic dipole interaction using the δM plot [24]. The observed slow relaxation can also be attributed to the thermal fluctuation of magnetization even after the atomic ordering under the weak intergranular magnetic dipole interaction [27]. Thermal fluctuation of magnetization is a serious problem for magnetic recording media, because it results in obscurity of the stored memory. From the viewpoint of high coercivity with high anisotropy, $L1_0$-FePt has a great possibility against the thermal fluctuation, but as the magnetic recording media, less intergrain interactions are also necessary. Also, it is said that too much coercivity owing to the huge anisotropy results in the poor overwrite performance [12].

Summary

Annealing of 2-dimentionally dispersed Fe/Pt nanoparticles on MgO and NaCl single crystal substrates at temperatures higher than 773 K leads to a formation of the ordered nanoparticles with mutual fixed orientation. Three variant ordered domains of the tetragonal $L1_0$ structure coexisted in single nm-sized FePt particle after annealing at 873 K. The magnetic coercivities varied depending on the annealing time at 873 K, the particle size and the measureing temperature. Even for the smallest averaged particle size of 8 nm, a high coercivity of about 3.5 kOe was observed. According to in-situ electron diffraction study, the degree of order of the FePt structure started to increase on annealing at 773 K and saturated on annealing at 873 K for 16 h. The magnetic hardening due to the atomic ordering was shown experimentally in nm-sized FePt particles.

The remanent magnetization decay curve showed a relation $\log M \propto -\log t$, and the slow relaxation expressed by this relationship could be explained due to the inter-granular magnetic dipole interaction.

Acknowledgements

The authors wish to thank Prof. T. Kawai and Dr. H. Tanaka of ISIR, Osaka University for support of the SQUID measurement. This study was supported by the Center of Excellence (COE) program of the Japanese Ministry of Education, Science, Sports and Culture.

References

1. R.L. White, R.M.H. New and R.F.W. Pease, IEEE Trans. Magn, 33[1] (1997) 990-995.
2. E.S. Murdock, IEEE Trans. Magn., 28[5] (1992) 3078-3083.
3. D.N. Lambeth, E.M.T. Velu, G.H. Bellesis, L.L. Lee and D.E. Laughlin, J. Appl. Phys., 79[8] (1996) 4496-4501.
4. M.H. Kryder, MRS Bull. 21[9] (1996) 17-19.
5. K. Ichihara, A. Kikitsu, K. Yusu, F. Nakamura and H. Ogiwara, IEEE Trans. Magn. 34[4] (1998) 1603-1605.
6. C. Chen, O. Kitakami and Y. Shimada: IEEE Trans. Magn. 35[5] (1999) 3466-3468.
7. S. Sung, C.B. Murray, D. Weller, L. Folks and A. Moser: Science 287 (2000) 1989-1991.
8. T.B. Massalski, H. Okamoto, P.R. Subramanian and L. Kacprzak (ed): Binary Alloy Phase Diagrams, 2nd ed. ASM International, Materials Park, Ohio, (1990) 1755.
9. A. Sakuma, J. Phys. Soc. Jpn. 63[8] (1994) 3053-3058.
10. T. Klemmer, D. Hoydick, H. Okumura, B. Zhang and W. A. Soffa, Scripta Met. Mater. 33[10/11] (1995) 1793-1805.
11. R.F.C. Farrow, D. Weller, R.F. Marks, M.F. Toney, A. Cebollada and G.R. Harp, J. Appl. Phys. 79[8] (1996) 5967-5969.
12. T. Shimatsu, J.C. Lodder, Y. Sugita and Y. Nakamura, IEEE Trans. Magn. 35[5] (1999) 2697-2699.
13. B. Bian, K. Sato, T. Ohkubo, Y. Hirotsu and A. Makino, J. Magn. Soc. Jpn. 23[1-2] (1999) 736-738.
14. C. Chen, O. Kitakami, S. Okamoto and Y. Shimada, J. Appl. Phys. 84[4] (1998) 2184-2188.
15. B.M. Lairson and B.M. Clemens, Appl. Phys. Lett. 63[10] (1993) 1438-1440.
16. M. Visokay and R. Sinclair, Appl. Phys. Lett. 66[13] (1995) 1692-1694.
17 S. Mitani, K. Takanashi, M. Sano, H. Fujimori, A. Osawa and H. Nakajima, J. Magn. Magn. Mater. 148[1-2] (1995) 163-164.
18. R.F.C. Farrow, D. Weller, R.F. Marks, M.F. Toney, S. Hom, G.R. Harp, A. Cebollada, Appl. Phys. Lett. 69[8] (1996) 1166-1168.
19. M. Watanabe and M. Homma, Jpn. J. Appl. Phys. 35[10A] (1996) L1264-L1267.
20. M.H. Hong, K. Hono and M. Watanabe, J. Appl. Phys. 84[8] (1998) 4403-4409.
21. B. Bian, K. Sato, Y. Hirotsu and A. Makino, Appl. Phys. Lett. 75[23] (1999) 3686-3688.
22. B. Bian, K. Sato, T. Ohkubo, Y. Hirotsu and A. Makino, J. Electron Microsc. 48[6] (1999) 753-760.
23. B. Bian, D.E. Laughlin, K. Sato and Y. Hirotsu, J. Appl. Phys. 87[9] (2000) 6962-6964.
24. B. Bian, D.E. Laughlin, K. Sato and Y. Hirotsu, IEEE Trans. Magn. (in press).
25. L. Néel, Ann. Geophys. 5 (1949) 99.
26. D.K. Lottice, R.M. White and E.D. Dahlberg, Phys. Rev. Lett. 67[3] (1991) 362-365.
27. Y. Park, S. Adenwalla, G.P. Felcher and S.D. Bader, Phys. Rev. B 52[17] (1995) 12779-12783.